Heavy and light hole minority carrier transport properties in low-doped n-InGaAs lattice matched to InP
Walker, Alexandre W.; Denhoff, Mike W.

National Research Council Canada   Conseil national de recherches Canada

Canada

Heavy and light hole minority carrier transport properties in low-doped n-InGaAs lattice matched to InP

Alexandre W. Walker[a] and Mike W. Denhoff

National Research Council of Canada, 1200 Montreal Road, M-50, Ottawa, Ontario K1A 0R6, Canada

Minority carrier diffusion lengths in low-doped n-InGaAs using InP/InGaAs double-heterostructures are reported using a simple electrical technique. The contributions from heavy and light holes are also extracted using this methodology, including minority carrier mobilities and lifetimes. Heavy holes are shown to initially dominate the transport due to their higher valence band density of states, but at large diffusion distances, the light holes begin to dominate due to their larger diffusion length. It is found that heavy holes have a diffusion length of $54.5 \pm 0.6\,\mu m$ for an n-InGaAs doping of $8.4 \times 10^{15}\,cm^{-3}$ at room temperature, whereas light holes have a diffusion length in excess of $140\,\mu m$. Heavy holes demonstrate a mobility of $692 \pm 63\,cm^2/Vs$ and a lifetime of $1.7 \pm 0.2\,\mu s$, whereas light holes demonstrate a mobility of $6200 \pm 960\,cm^{-2}/Vs$ and a slightly longer lifetime of $2.6 \pm 1.0\,\mu s$. The presented method, which is limited to low injection conditions, is capable of accurately resolving minority carrier transport properties. © 2017 Author(s). All article content, except where otherwise noted, is licensed under a Creative Commons Attribution (CC BY) license (http://creativecommons.org/licenses/by/4.0/). https://doi.org/10.1063/1.5002677

Minority carrier diffusion lengths are critically influential in optoelectronic device performance, for example, solar cells, photodetectors, and heterojunction bipolar transistors. Several methods presently exist to measure these, including electron beam induced current (EBIC) along a cross-sectional *pn* junction,[1] cathodoluminescence (CL) measurements on double-heterostructures,[2–4] zero-field time-of-flight,[5,6] and surface photovoltage[7,8] to name a few. Coupling these diffusion lengths to lifetime measurements typically obtained from time-resolved photoluminescence, time-of-flight experiments, or time-resolved CL measurements,[9] one can then infer minority carrier mobilities if both measurements are performed for a comparable excess carrier concentration. These parameters can be critical in designing minority carrier devices, for example, in cases where minority carrier mobilities exceed majority carrier mobilities[6] or in solar cells where minority carrier diffusion lengths are on the order of the active region thickness.[10]

Each of the aforementioned methodologies has its inherent advantages and disadvantages. For example, the zero-field time-of-flight method is simple in principle but becomes obfuscated when fitting the transient photovoltage for a heterojunction such as an InP/InGaAs photodetector. For cross-sectional EBIC, the method can be destructive since samples must be well polished for a clean cross-section, and the requirement of an electron microscope can result in significant time and effort. Thus, it is of interest to develop an overall simpler method to measure minority carrier diffusion lengths. Here, we present a purely electrical method capable of extracting diffusion lengths. The method is demonstrated using an n-type InP:Si/intrinsic InGaAs/n-type InP:Si double-heterostructure which is used to make *pin* short wave infrared detectors and focal plane arrays.[11] Furthermore, this method is shown to be capable of separating the contributions of heavy

and light holes, and, with a few assumptions, determining the lifetimes and diffusion constants (i.e., mobilities). The required test devices can also be included on production wafers to monitor the material and fabrication quality across the wafer and from epitaxial run to run. These test structures consist of long ($750\,\mu m$) and thin ($10\,\mu m$) diffused junction line diodes as shown in Fig. 1. The junction is created by Zn diffusion through the InP and about 100 nm into the InGaAs material. The inter-line diode separations range from much shorter to much longer than the diffusion length. Note that, during the measurement, one can bypass one diode to obtain a larger distance, as illustrated by d_6 in Fig. 1.

The basic physics is summarized in detail elsewhere.[11,12] Essentially, forward biasing one line diode injects minority carriers into the InGaAs layer leading to diffusion of carriers through the InGaAs channel. This can be seen in Fig. 2 that shows a simulated cross-section of the device in terms of the hole concentration as a function of depth and lateral position between two adjacent line diodes using Atlas by Silvaco (v.5.23.12.C), assuming default material properties.[13] The
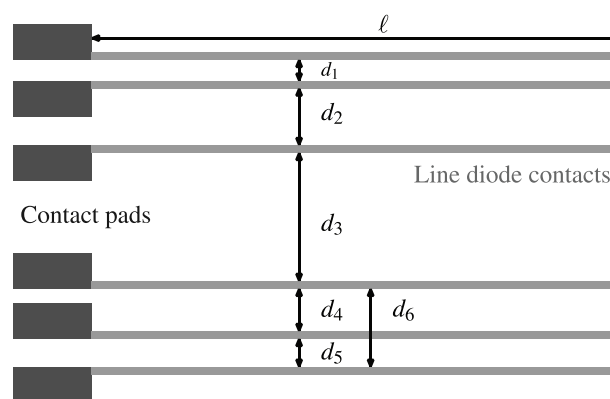

FIG. 1. Set of long and thin diffused junction diodes with inter-diode spacings $d_{1..6}$, where the diode length $\ell \gg d_{1..6}$.

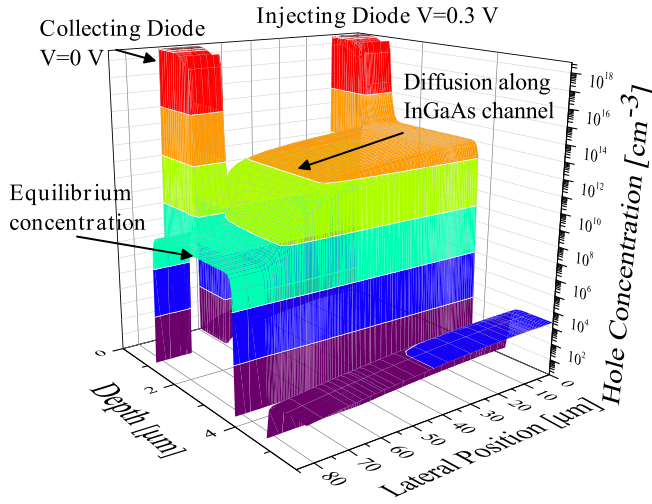[a]Electronic mail: alexandre.walker@nrc-cnrc.gc.ca

FIG. 2. Simulated carrier concentration as a function of depth in device and lateral distance between two adjacent diodes using Atlas (v5.23.12.C) by Silvaco. Regions of very low hole concentration correspond to InP. The red to violet color coding represents the magnitude of the carrier concentration.

hole concentration is uniform across the thickness of the InGaAs layer since its thickness ($2.7\,\mu m$) is significantly smaller than the diffusion length. The carriers which diffuse to an adjacent line diode are collected by applying a zero or slightly reverse bias with respect to the bottom InP layer which serves as the ground contact. Assuming low injection, if the length of the line diode ℓ is sufficiently long compared to the maximum interdiode distance d_i, and if d_i is much longer than the InGaAs thickness, the hole current can be described by the one dimensional diffusion equation. The hole density under the injecting diode is p_{inj}, which is dictated by the applied bias, and the hole concentration at the collecting diode is the equilibrium value p_0 since the collecting diode is maintained at zero applied bias. Using these boundary conditions and assuming no interface recombination, solving the diffusion equation leads to the solution in terms of the collected hole current density $J_p(W)$ as a function of interdiode separation W given as[11,12]

$$J_p(W) = \frac{qD(p_{inj} - p_0)}{L\sinh(W/L)},\qquad(1)$$

where L is the diffusion length, $D = \mu k_B T/q$ is the diffusion coefficient, μ is the mobility, k_B is Boltzmann's constant, T is the temperature, and q is the electronic charge. In the case of low injection, the initial (injected) hole density p_{inj} can be calculated using $p_{inj} = n_i^2/N_D \exp(qV/k_B T)$, where n_i is the intrinsic carrier concentration and $N_D = 8.4 \times 10^{15}\,cm^{-3}$ is the donor concentration in the InGaAs extracted using CV measurements on $200\,\mu m$ diameter devices. Finally, p_0 is the equilibrium hole concentration given by $p_0 = n_i^2/N_D$. Note that the cross-sectional area used to scale the measured current to a current density is given by $A = t \times \ell$, where t is the InGaAs thickness and ℓ is the length of the diode. Fitting Eq. (1) to experimental data thus reveals the minority carrier diffusion length L and the mobility μ, thus giving access to the lifetime τ. An electron effective mass of $0.043\,m_e$ is assumed for InGaAs, along with heavy and light hole effective masses of $0.46\,m_e$ and $0.047\,m_e$, respectively, and a room temperature

bandgap of $0.734\,eV$.[14] This gives an intrinsic carrier concentration of $n_i = 6.14 \times 10^{11}\,cm^{-3}$ for room temperature ($T = 296\,K$).

However, an important consideration that is easy to overlook is the interdiode separation W. The simulation results of Fig. 2 show that the hole concentration is nearly constant under the injecting diode but starts decreasing by 1%–2% within $\sim 1\,\mu m$ of the inside edge of the diode. On the other hand, the hole concentration drops rapidly to the equilibrium concentration from the leading edge of the collecting diode. The separation of the diodes therefore starts a small distance inside the edge of the injecting diode and ends some distance past the leading edge of the collecting diode. This separation correction, δ, to the interdiode separation W, defined from the inner edges of two diodes, is discussed later.

Current-voltage measurements were made using a Hewlett-Packard HP4155C Semiconductor Analyzer. The results from devices from two different wafers than the device reported here were reported in Ref. 11 and are similar to the present results. A fit to measured collected current densities for an applied bias of $0.3\,V$ to Eq. (1) with fitting parameters $L = 66.6\,\mu m$ and $D = 23.5\,cm^2/s$ is shown in the inset of Fig. 3, assuming a separation correction of $\delta = 2.5\,\mu m$. The measured collected current for the largest separation of $330\,\mu m$ is well above the theoretical fit, and the point at $210\,\mu m$ is also above, albeit slightly. These higher than expected currents at large diffusion distances can be explained by the existence of light holes with a longer diffusion length than heavy holes.

In order to account for both heavy and light holes, two versions of Eq. (1), one for heavy holes and one for light holes, can be added together to give the total collected current. The number of fitting parameters doubles, which can lead to more ambiguity in the fit. One must first calculate the fraction of the injected hole concentration composed of heavy holes, f_{HH}, which is dictated by the ratio of heavy hole density of states to the total valence band density of states N_v (ignoring the split-off band), given as
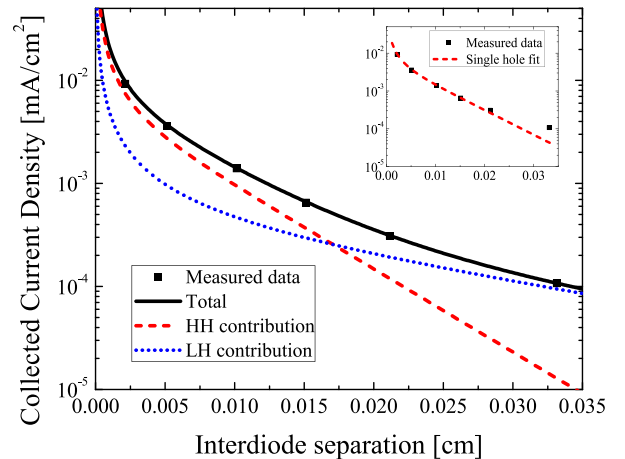

FIG. 3. Measured collected current density as a function of interdiode separation W for $V = 0.3\,V$, including the best-fit to Eq. (1) for light and heavy holes and the sum of both terms. The inset shows the fit according only to a single hole type.

$$f_{HH} = \frac{N_v^{HH}}{N_v^{HH} + N_v^{LH}} = \frac{m_{HH}^{3/2}}{m_{HH}^{3/2} + m_{LH}^{3/2}}; \qquad (2)$$

the fraction for light hole occupation is analogous, or simply given as $f_{LH} = 1 - f_{HH}$. For the adopted heavy and light holes effective masses, heavy holes dominate the valence band density of states by a factor of ~30.

The best fit of Eq. (1) for the sum of heavy and light holes, as well as their individual contributions, is illustrated in Fig. 3 for an applied bias of 0.3 V. The fit is achieved using a nonlinear least squares fitting algorithm from Matlab R2017a's curve fitting toolbox. The algorithm uses the diffusion length and diffusion constant for both light and heavy holes, respectively, as fitting parameters. Standard errors for the best-fit parameters are computed using the mean square errors and the Jacobian matrix at the solution (i.e., neglecting the higher order terms to approximate the Hessian matrix, which is reasonable since the residuals are close to zero at the solution). It is clear that adding a term specifically for the light holes yields a much better agreement for the largest interdiode separations. The heavy and light hole diffusion lengths are extracted to be $53.9 \pm 0.8\,\mu m$ and $192 \pm 22\,\mu m$, respectively, again assuming a separation correction of $\delta = 2.5\,\mu m$. These can be compared to the diffusion length of $66.6\,\mu m$ found using the single carrier model. This single carrier value thus represents an effective diffusion length, combining both a shorter heavy hole diffusion length and a longer light hole diffusion length. These diffusion lengths are within the range of previously determined diffusion lengths of $140\,\mu m$ at room temperature for a lower doping of $10^{15}\,cm^{-3}$.[15] From the results in Fig. 3, for short interdiode separations, the current is mainly due to heavy holes; in particular, for $W = 0$, ~80% of the current is due to heavy hole transport. This decreases to 50% at $200\,\mu m$, beyond which light holes dominate the transport. For minority carrier devices such as InGaAs/InP pnp transistors, light holes can contribute ~20% of the diffusion current.

It is now important to discuss the influence of the separation correction to the interdiode separation W on the extracted diffusion length. For example, setting this to $\delta = 0.5\,\mu m$ results in a heavy hole $L = 58.6 \pm 3.5\,\mu m$ (a 9% increase) and light hole $L = 248 \pm 190\,\mu m$ (a 30% increase); note the large uncertainties. Exceeding $2.5\,\mu m$ further decreases the diffusion lengths but also increases the uncertainties. A value of $2.5\,\mu m$ is thus used in the remaining analysis and is assumed to be constant as a function of separation.

The fitting can be performed as a function of voltage to investigate the injection level dependence of the diffusion lengths for this sample. This also tests the ability of the method to extract consistent parameters. The results are illustrated in Fig. 4, where the applied bias is shown on the bottom axis and the corresponding injected hole concentration is shown on the top axis. One can observe a near constant diffusion length across the voltage range of 0.2–0.4 V for the heavy holes, which validates the robustness of the method. The light holes, however, show a trend of increasing diffusion length for increasing voltage, although it could be considered constant within the error bars. This may be due to the choice of the separation correction value and/or by
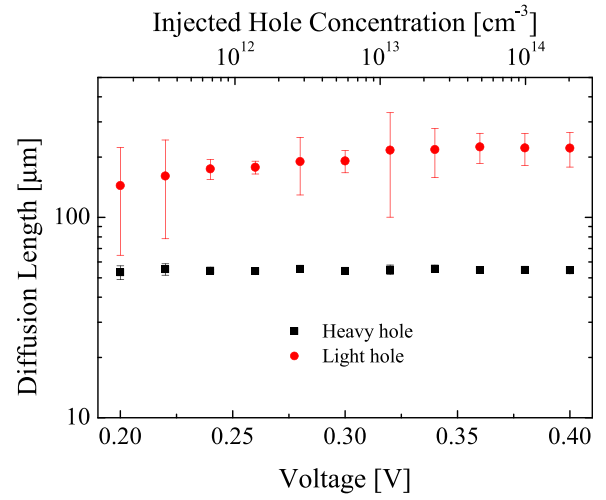

FIG. 4. Extracted hole diffusion length in n-InGaAs as a function of applied bias on a logarithmic scale (injected hole concentration shown on the top axis).

assuming that it is constant as a function of separation. It is further complicated by the random error in the current measurement. Improving the determination of the W correction factor requires further investigation using careful device simulations. The standard deviation for heavy hole diffusion lengths ($<\%$) is significantly smaller than for light holes (~25%). This is due to the heavy hole parameter fitting being based on sufficient data points, whereas light hole parameters rely mainly on the last two data points. More data points for larger interdiode separations would improve the accuracy of the extracted light hole diffusion lengths, and this may clarify the observed trend of increasing L for increasing voltage. Lastly, the standard error is observed to vary considerably depending on the fit (even if it appears good by eye), and this is due to current measurement errors. Overall, the light hole diffusion lengths are ~3 × longer than the heavy hole diffusion lengths, which is a result of the larger light hole mobility (discussed next). Also, increasing the hole injection beyond $V > 0.4\,V$ leads to a breakdown of the model's low injection assumption. Lastly, fitting at sufficiently low voltage ($V < 0.2\,V$) results in large uncertainties due to the significant scatter in the data arising from hysteresis in the current measurement and the overall high noise in measuring currents below 10 pA. Improving the accuracy of the current measurement would result in more accurate diffusion length parameters.

The minority carrier mobilities are also obtained as a function of voltage from the fit to the data. The results are illustrated in Fig. 5(a). The average mobilities are 692 ± 63 and $6200 \pm 960\,cm^2/Vs$ for heavy and light holes, respectively. The observed trends of decreasing mobility for increasing voltage were not expected. Further investigation into this is required to determine if this observation is real. Note that the mobility results depend strongly on the choice of band parameters (which dictate the calculated injection level) and temperature. The choice of separation correction δ primarily influences the light hole transport properties. Nevertheless, light holes are determined to be significantly more mobile than heavy holes by a factor of ~9, which is expected based on their effective masses as well as their
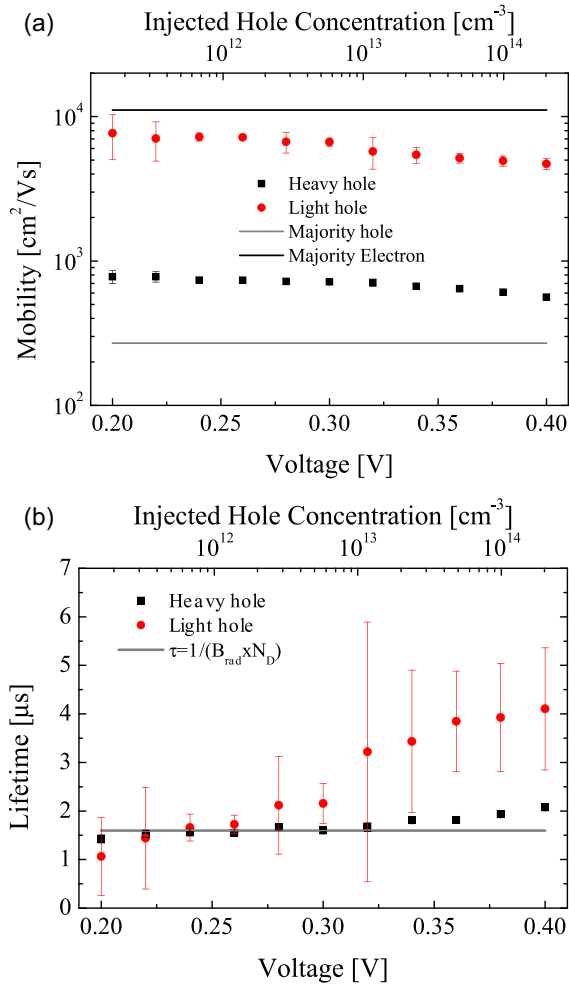
FIG. 5. Extracted (a) mobility (on a logarithmic scale) and (b) lifetime for heavy and light holes as a function of injection. Mobility plots include the majority electron and hole Hall mobilities[16] for the InGaAs doping of $N_D = 8.4 \times 10^{15} \text{cm}^{-3}$. The lifetime plot shows the expected radiative lifetime according to $\tau = \frac{1}{B_{rad}N_D}$, where $B_{rad} = 0.75 \times 10^{-10} \text{ cm}^{-3}/\text{s}$.

extracted diffusion lengths. The light hole mobility is somewhat smaller but on the same order of magnitude as the electron Hall mobility ($\sim 14\,000 \text{ cm}^2/\text{Vs}$) for the intrinsic material,[16] considering their similar effective masses. Interestingly, the heavy hole mobilities are considerably larger than the majority hole Hall mobility of $269 \text{ cm}^2/\text{Vs}$ for the corresponding sample doping level of $8.4 \times 10^{15} \text{ cm}^{-3}$.[16] Overall, the heavy and light hole mobilities fall within the range of hole and electron mobilities from Sotoodeh [see horizontal lines in Fig. 5(a)]. With respect to other published data, the hole mobility reported here is greater than the $425 \text{ cm}^2/\text{Vs}$ value reported by Gallant and Zemel.[15] This emphasizes the importance of characterizing minority carrier mobilities for device design and simulation. Overall, careful temperature control is critical for this component of the study. Lastly, a better knowledge of band parameters would improve the extraction of the mobilities.

Finally, Fig. 5(b) illustrates the extracted lifetimes for heavy and light holes as a function of injection. The heavy hole lifetime corresponds to the lifetime dictated by the radiative recombination coefficient $B_{rad} = 0.75 \times 10^{-10} \text{ cm}^3/\text{s}$ and the doping, indicated by the horizontal line. This is in agreement with other studies conducted on low-doped

InGaAs.[11,17–19] While technically this method cannot distinguish between bulk recombination in the layer and surface recombination at the hetero junction interfaces, the apparent dominance of radiative recombination justifies the assumption of negligible surface recombination. The lifetimes for heavy holes are more accurate than those for light holes. For the device reported here, as well as other devices, the light hole lifetime appears to be longer than for heavy holes. Again, more data in the range of the largest interdiode separations would be required to improve the accuracy of the lifetime for the light holes. An independent measurement of the effective lifetime (both heavy and light holes) could also reduce the fitting parameters, thereby potentially providing better results for the diffusion length and mobility.

In conclusion, a simple and nondestructive electrical method was proposed to extract minority carrier diffusion lengths, mobilities, and lifetimes using long and thin diffused double-heterostructure diodes. The proposed method was demonstrated in low-doped n-InGaAs lattice matched to InP for a sample doped to $8.4 \times 10^{15} \text{ cm}^{-3}$. Heavy and light hole diffusion was observed as separate contributions, with a heavy hole diffusion length of $54.4 \pm 0.6 \, \mu\text{m}$ (averaged over injection) and a light hole diffusion length of $195 \pm 26 \, \mu\text{m}$. The hole mobilities were extracted to be 692 ± 63 and $6200 \pm 960 \text{ cm}^2/\text{Vs}$ for heavy and light holes, respectively. Ultimately, radiative recombination dominates the lifetime component, which is found to be $1.7 \pm 0.2 \, \mu\text{s}$ for heavy holes and $2.6 \pm 1.0 \, \mu\text{s}$ for light holes. The method is limited to low injection and to diffusion lengths longer than the InGaAs layer thickness.

[1]S. I. Maximenko, M. P. Lumb, R. Hoheisel, M. Gonzalez, D. A. Scheiman, S. R. Messenger, T. N. D. Tibbits, M. Imaizumi, T. Ohshima, S. I. Sato, P. P. Jenkins, and R. J. Walters, "Radiation response of multi-quantum well solar cells: Electron-beam-induced current analysis," J. Appl. Phys. **118**, 245705 (2015).

[2]F. J. Schultes, T. Christian, R. Jones-Albertus, E. Pickett, K. Alberi, B. Fluegel, T. Liu, P. Misra, A. Sukiasyan, H. Yuen, and N. M. Haegel, "Temperature dependence of diffusion length, lifetime and minority electron mobility in GaInP," Appl. Phys. Lett. **103**, 242106 (2013).

[3]M. Niemeyer, J. Ohlmann, A. W. Walker, P. Kleinschmidt, R. Lang, T. Hannappel, F. Dimroth, and D. Lackner, "Minority carrier diffusion length, lifetime and mobility in p-type GaAs and GaInAs," J. Appl. Phys. **122**, 115702 (2017).

[4]A. Gustafsson, J. Bolinsson, N. Skold, and L. Samuelson, "Determination of diffusion lengths in nanowires using cathodoluminescence," Appl. Phys. Lett. **97**, 072114 (2010).

[5]A. K. Sharma, S. N. Singh, N. S. Bisht, H. C. Kandpal, and Z. H. Khan, "Determination of minority carrier diffusion length from distance dependence of lateral photocurrent for side-on illumination," Sol. Energy Mater. Sol. Cells **100**, 48–52 (2012).

[6]M. L. Lovejoy, M. R. Melloch, M. S. Lundstrom, and R. K. Ahrenkiel, "Temperature dependence of minority and majority carrier mobilities in degenerately doped GaAs," Appl. Phys. Lett. **67**(8), 1101–1103 (1995).

[7]D. K. Schroder, "Surface voltage and surface photovoltage: History, theory and applications," Meas. Sci. Technol. **12**, R16–R31 (2001).

[8]L. Kronik and Y. Shapria, "Surface photovoltage phenomena: Theory, experiment and applications," Surf. Sci. Rep. **37**, 1–206 (1999).

[9]M. Boulou and D. Bois, "Cathodoluminescence measurements of the minority-carrier lifetime in semiconductors," J. Appl. Phys. **48**, 4713 (1977).

[10]A. W. Walker, S. Heckelman, T. Tibbits, D. Lackner, A. W. Bett, and F. Dimroth, "Radiation hardness of AlGaAs n-i-p solar cells with higher bandgap intrinsic regions," Sol. Energy Mater. Sol. Cells **168**, 234–240 (2017).

[11]A. W. Walker and M. Denhoff, "Minority carrier diffusion lengths and mobilities in low-doped InGaAs for focal plane array applications," Proc. SPIE **10177**, 101772D (2017).

[12]S. M. Sze, *Physics of Semiconductor Devices*, 3rd ed. (Wiley, New York, 2007), p. 66.

[13]Silvaco, Inc., *Atlas User's Manual, Device Simulation Software* (Santa Clara, CA, USA).

[14]I. Vurgaftman, J. R. Meyer, and L. R. Ram-Mohan, "Band parameters for III-V compound semiconductors and their alloys," J. Appl. Phys. **89**, 5815 (2001).

[15]M. Gallant and A. Zemel, "Long minority carrier diffusion length and evidence for bulk radiative recombination limited lifetime in InP/InGaAs/InP double heterostructures," Appl. Phys. Lett. **52**, 1686 (1988).

[16]M. Sotoodeh, A. H. Khalid, and A. A. Rezazadeh, "Empirical low-field mobility model for III-V compounds applicable in device simulation codes," J. Appl. Phys. **87**, 2890 (2000).

[17]A. R. Wichman, R. E. DeWames, and E. Bellotti, "Three-dimensional numerical simulation of planar P+n heterojunction $In_{0.53}Ga_{0.47}As$ photodiodes in dense arrays Part I: Dark current dependence on device geometry," Proc. SPIE **9070**, 907003 (2014).

[18]E. Zielinski, H. Schweizer, K. Streubel, H. Eisele, and G. Weimann, "Excitonic transitions and exciton damping processes in InGaAs/InP," J. Appl. Phys. **59**, 2196 (1986).

[19]E. Wintner and E. P. Ippen, "Nonlinear carrier dynamics in $Ga_xIn_1xAs_yP_{1y}$ compounds," Appl. Phys. Lett. **44**, 999 (1984).